ATOMRISTORS: NON-VOLATILE RESISTANCE SWITCHING IN 2D MONOLAYERS

Xiaohan Wu, Ruijing Ge, Myungsoo Kim, Deji Akinwande and Jack C. Lee
University of Texas at Austin
TX, USA
xiaohan_wu@utexas.edu, ruijing@utexas.edu, myungsoo.kim@utexas.edu, deji@ece.utexas.edu and leejc@austin.utexas.edu

ABSTRACT
Since the discovery of graphene, two-dimensional (2D) materials have drawn much attention as a promising candidate in the next-generation electron devices, optoelectronics and bioelectronics[1, 2]. Over the last few years, researchers have proved the existence of the non-volatile resistance switching (NVRS) behavior in various 2D materials, including graphene oxide, functionalized MoS_2, partially degraded black phosphorus and multi-layer hexagonal boron-nitride (h-BN), etc. [3-6], where the resistance can be switched between a high-resistance state (HRS) and a low-resistance state (LRS) and maintained for a long time without power supply [7]. In 2015, Sangwan et al. discovered that grain boundaries in single-layer MoS_2 can produce NVRS based on planar (horizontal) structure [8]. However, the planar structure without 3D stacking ability has the limitation of low integration density. Therefore, to overcome vertical scaling obstacle in NVRS based on conventional metal-insulator-metal (MIM) structure, it is desired to find out the thinnest materials that can produce the resistance switching behavior based on vertical device structure.

Recently, we discovered that NVRS phenomenon is accessible in a variety of single-layer transition metal dichalcogenides (TMDs) and single-layer h-BN in vertical MIM configuration [9-12]. Compared with other 2D material-based NVRS devices, single-layer h-BN has only one atomic layer and ~0.33 nm in thickness, which is the thinnest active layer in non-volatile resistance memory. These devices can be collectively labelled as "atomristor", which means the memristor effect in atomically thin nanomaterials. The TMDs and h-BN atomristors have been studied using a crossbar or a litho-free & transfer-free structure, demonstrating forming-free switching with large on/off ratio (up to 6 orders of magnitude) and low switching voltage (down to < 1V). In addition, the devices are proved via pulse operation with fast switching speed (< 15 ns), which is comparable to the state-of-the-art speed in 2D memristors. The non-volatile RF switches based on h-BN atomristors are realized with low insertion loss (< 0.2 dB) and high isolation (> 15 dB) up to 100 GHz. The operating frequencies cover the RF, 5G, and mm-wave bands, making this a promising low-power switch for diverse communication and connectivity front-end systems. The results of this work indicate a potential universal resistive switching behavior in 2D monolayers, which is applicable to memory technology, neuromorphic computing, RF switch and flexible electronics.

Key words: two-dimensional materials, non-volatile memory, transition metal dichalcogenides, hexagonal boron nitride, resistance switching, RF switch.

INTRODUCTION
Two-dimensional materials have been studied in the last decade as the most attractive materials beyond silicon. In 2004, Andre Geim and Konstantin Novoselov at the University of Manchester discovered, isolated and characterized the first two-dimensional material, graphene, which consists of only a single layer of atoms[13]. The remarkable electronic, optical, mechanical and thermal properties have drawn significant attentions and subsequently inspired more and more 2D materials to be discovered and analyzed, including transition metal dichalcogenides (TMDs), diatomic hexagonal boron nitride (h-BN), and emerging monoatomic buckled crystals Xenes, which include silicene, germanene and phosphorene[1]. The 2D atomic sheets are defined as atomically thin, layered crystalline solids with the characteristics of intralayer covalent bonding and interlayer van der Waals bonding. These materials are considered 2D as they represent the thinnest unsupported crystalline materials that can be realized. Now the collection of 2D materials has been expanded to hundreds or expectedly thousands due to more elemental and compound sheets uncovered. With that being considered, semiconductor industry can largely benefit from the new atomically thin materials with more applications in development.

Graphene has been utilized in electronics devices mainly as the conductive electrodes since it is a zero-gap semiconductor – its conduction and valence bands meet at the Dirac points. The material shows remarkable electron mobility at room temperature with reported values in excess of 15000 $cm^2 V^{-1} s^{-1}$. However, the zero-gap nature limits its applications in field effect transistors (FET). MoS_2, as a representative TMD monolayers, has ~1.8 eV direct band gap, thus is suitable to be used in FET devices[14]. In addition, hexagonal boron nitride (h-BN) also stands out among other 2D materials as a high band gap insulating material at ~ 5.9 eV, which makes it perfect for the production of ultrahigh mobility 2D heterostructures composed of various types of 2D semiconductors[15].

Non-volatile memory (NVM) has long been the focus in both academia and industry[16]. In contrast to volatile memory, such as dynamic random access memory (DRAM) or static random access memory (SRAM), where data will be quickly lost if power is interrupted, the non-volatile memory can retrieve the stored information even without any power supply. The volatile memory is usually used as the primary storage while non-volatile memory is used as the secondary storage or long-term persistent storage. We are in an era of the explosion of the data. Thus, a massive amount of data needs to be stored and analyzed, which inspires the research of advanced high-density, high-speed non-volatile memory. The most commonly used non-volatile memory is flash memory, which also represents the big market of solid-state drive (Fig. 1). Flash memory devices use two different technologies – NOR and NAND – to map data. The NOR flash provides high-speed random access, reading and writing data in specific memory location, thus retrieving as little as a single byte. While NAND flash reads and writes sequentially at high speed, handling data in blocks, but relatively slower on read if compared with NOR. Flash memory is based on a modified metal-oxide-semiconductor field-effect transistor, known as floating-gate MOSFET, where an additional electrically isolated gate is inserted between the channel and control gate. Adding or removing charges within the floating gate can change the threshold voltage, thereby defining whether the cell is in a programmed or erased state. Although the flash memory has advantages of fast read and write speed, low power consumption and prone to damage compared with traditional hard disk drives, it still has some drawbacks such as limited endurance and retention for smaller device and the problems in the transistor structure. To find the next-generation non-volatile memory to replace flash memory, researchers have been working on various emerging non-volatile memory, including ferroelectric random access memory (FeRAM), phase change memory (PCM), spin-transfer torque magnetic random access memory (STT-MRAM) and resistive random access memory (RRAM).

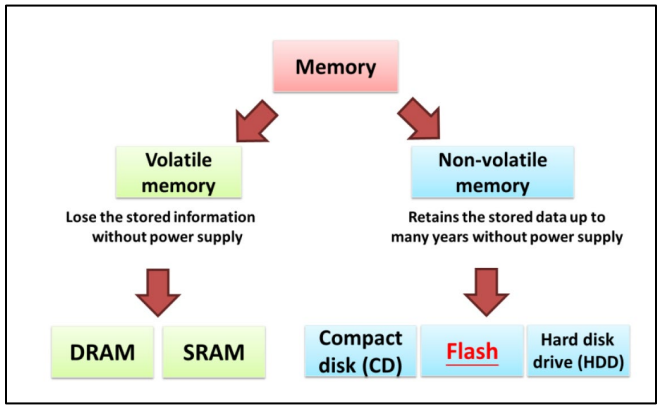

Figure 1. Memory categorized into volatile memory and non-volatile memory.

Among those candidates, the RRAM devices exhibit excellent endurance and retention compared with flash memory, and show lower power consumption, faster switching speed and better scalability[7]. The structure of a RRAM device is very simple, basically metal-insulator-metal (MIM) stacking. The resistor-like structure not only takes up less die space therefore enabling higher memory density and lower memory unit price, but also promises a more straightforward multi-level staking scheme to construct 3D memory. The traditional insulating material in RRAM is bulk metal oxides, such as TiO_2 or HfO_2. With external electrical bias, a conductive filament will be formed in the insulator. Depending on the formation and rupture of the conductive filament, the device can be switched between a high-resistance state (HRS) and a low-resistance state (LRS). This is the non-volatile resistance switching (NVRS) phenomenon. Recently, more works have been done in the development of RRAM devices not only in memory application but also in neuromorphic computing because of its analog-like multi-state switching behavior.

In the last few years, as the continuous study on 2D materials, it has been found that several 2D materials also exhibit NVRS phenomenon, expanding the categories of NVRS materials to the ultrathin layered crystalline films. As we all know, graphene is a zero-gap semiconductor. Thus, it is not a suitable material for resistance switching devices. Graphene oxide, on the other hand, can be successfully used as the active layer in NVRS devices[17]. As for the semiconducting 2D materials, MoS_2 has been found to work in memristors in the form of 1T phase[18]. Moreover, Sangwan et al. discovered that grain boundaries in single-layer MoS_2 can produce NVRS based on planar (horizontal) structure[8]. Another example is h-BN, a representative 2D insulator, which has been reported to show the NVRS behavior in multilayer nanosheets[6]. However, the monolayer 2D materials are not found to show resistance switching in vertical MIM configuration.

In our work, we first reported the discovery of NVRS phenomenon in monolayer 2D materials in vertical device structure, including TMDs (MoS_2, $MoSe_2$, WS_2 and WSe_2) and h-BN. The devices feature forming-free bipolar and unipolar switching, with relatively low switching voltages down to < 1V. In addition, a large on/off current ratio of more than 10^6 can be obtained in these devices, which enables potential applications in multi-bit storage and neuromorphic computing. Besides DC operation, pulse can be applied to switch the device with fast switching speed (< 15 ns). By using the monolayer TMDs and h-BN, it is proved that NVRS can be accessed in 2D monolayers in vertical device structure (the devices can be collectively labeled as atomristors), which inspires the experimental and theoretical research of resistance switching in the intrigued atomically thin crystalline sheets. Moreover, the record thinness of NVRS materials is reduced to ~ 0.33 nm of single-layer h-BN with only one atomic layer. Compared with traditional flash memory using 2D materials, the resistance switching memory devices have the advantage of lower switching voltage and overcomes the problem of leakage of stored charges in the floating gate through the tunneling oxide for small-area devices, which enables high integration density.

Benefit from the ultra-thin nature of the active layer, a novel application, RF switch, is realized based on the atomristors. The non-volatile RF switch low insertion loss (< 0.2 dB) and high isolation (> 15 dB) up to 100 GHz. The operating frequencies cover the RF, 5G, and mm-wave bands, making this a promising low-power switch for diverse communication and connectivity front-end systems.

2D CVD MATERIALS PREPARATION

CVD-grown monolayer MoS_2 were grown on SiO_2/Si substrates using sulfur and MoO_3 as precursors at 850 °C for 5 minutes[19]. Some monolayer MoS_2, $MoSe_2$, WS_2 and WSe_2 samples were grown at 500 °C for 24 hours by wafer-scale MOCVD. Molybdenum hexacarbonyl ($Mo(CO)_6$, MHC, Sigma Aldrich 577766), tungsten hexacarbonyl ($W(CO)_6$, THC, Sigma Aldrich 472956), diethyl sulphide ($C_4H_{10}S$, DES, Sigma Aldrich 107247) and dimethyl selenide were the chemical precursors for Mo, W, S and Se respectively. The growth of monolayer MoS_2 on Au foil was performed in a multitemperature-zone tubular furnace (Lindberg/Blue M) equipped with a 1-in.-diameter quartz tube. The sulfur powder was placed outside the hot zone, sublimated at ~102 °C, and then carried to the downstream growth zone by Ar gas (50 standard cubic centimeter per minute (sccm)). The MoO_3 powders (Alfa Aesar, purity 99.9%) and Au foils (Alfa Aesar, purity 99.985%, thickness ~25 μm) were then placed on the downstream region of the quartz tube. The MoO_3 powders were heated from room temperature to ~530 °C within 30 min with a heating rate of ~17 °C/min. The growth pressure on Au foils was set at 30 Pa, and the growth time for 60 min at 750 °C.

CVD h-BN was grown by CVD on Ni foil substrates, which was folded into a Ni enclosure[20, 21]. Ammonia borane powder precursor was heated separately above its decomposition temperature. The precursor was carried by 5 sccm H_2 to the substrate in the furnace at 1050 °C. The process used was a carbo-thermal reduction process where another 5 sccm CH_4 gas was also flowed. The carbon does not incorporate into the h-BN, but rather helps to reduce boron oxide. After 5 minutes, the furnace and the methane and ammonia borane sources were shut, and the sample was cooled under 5 sccm H_2. The total pressure of the system during synthesis was roughly 200 mTorr.

Low pressure chemical vapor deposition (LPCVD) method was used to directly grow monolayer h-BN on Au foils[22]. Firstly, commercial Au foils with thickness of 25 μm were sequentially cleaned in HCl solution, acetone and distilled water for ~10 min using ultrasonic cleaner. Further high temperature annealing (950 °C for 5 h) in the air condition was induced to improve the crystallinity and flatness of the Au foils. Secondly, the pre-treated foils were placed into a tube furnace chamber for the growth of h-BN. The chamber was pumped to 0.5 Pa and then a mixture flow of 200 sccm H_2 and 80 sccm Ar were flown in the chamber as carrier gases. After high temperature annealing for 60 min at 1030 °C, ammonia borane vapor was mixed into the carrier gases as the h-BN feedstocks for 10 min. Finally, the temperature of chamber was naturally cooled down to room temperature.

DEVICE FABRICATION AND MEASUREMENT

The crossbar device fabrication started with bottom electrodes (BE) patterning by electron beam lithography and 2 nm Cr/60 nm Au metal stack deposition on an SiO_2/Si (285 nm) substrate. The litho-free device used global electrode (2nm Cr/60nm Au) as BE and pure Au for the TE. Single-layer TMD was then transferred onto the fabricated substrate using resist-free polydimethylsiloxane (PDMS) stamp transfer method. In this transfer process, monolayer TMD was brought into conformal contact with PDMS. Then substrate-TMD-PDMS system was soaked into diluted water. Since the original substrate (SiO_2) is hydrophilic, it is easy for water to diffuse into the TMD-substrate interface, which helps separate the two layers. The PDMS-TMD film was then brought into contact with the target fabricated substrate. The PDMS stamp was subsequently peeled off to leave monolayer TMD films on the target substrate. CVD h-BN was transferred onto BE from the Ni foil substrate using a poly(methyl methacrylate) (PMMA)-assisted wet transfer method. A thin layer of PMMA was spin coated onto the h-BN/Ni and then the Ni was etched away in 0.5 M ammonia persulfate solution. The PMMA/h-BN was rinsed in DI water to remove any etchant by-product prior to lifting by the target substrate with BE. The PMMA was then removed by immersing in acetone. For crossbar devices, top electrodes (TE), using the same fabrication process as BE, was patterned and deposited. While for the litho-free device, the TE (60nm Au) was deposited via a shadow mask. The devices were measured on a Cascade or Lakeshore probe station with an Agilent 4156 semiconductor parameter analyzer under ambient conditions. The pulse measurements were conducted using a Keithley 4200A-SCS parameter analyzer. Microwave switch performance was characterized up using an Agilent two-port network analyzer.

RESULTS AND DISCUSSION

DC electrical measurements were performed on the crossbar devices which consist of monolayer MoS_2 sheets between Au bottom and top electrodes, revealing non-volatile resistance switching behavior (Fig. 2). In a typical I-V curve, the resistance switching can be described as follows. First, the as-fabricated device is at a high-resistance state (HRS). An

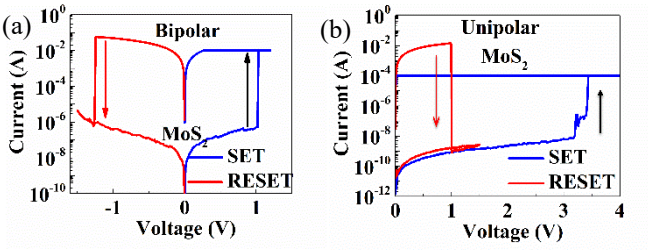

Figure 2. Bipolar and unipolar I-V curves of the monolayer MoS_2 atomristors.

external electrical bias is given to the device. At ~1 V, the current suddenly increases to the compliance, indicating a switching from the high resistance state to the low-resistance

state (LRS). This transition is what we called a SET process. The resistance state can be retained without power supply for a long time, showing the non-volatility of the switching. To switch back to HRS, in a bipolar device (Fig. 2a), a reverse bias is applied to the device. At ~ -1.25V, the current suddenly decreases, indicating a transition from the LRS to HRS (RESET process). For a unipolar device (Fig. 2b), the RESET and SET process are in the same direction of voltage bias. Similarly, the HRS can be maintained without external power. The device can be repeatably switched between the HRS and LRS. Unlike most of traditional NVRS devices that use metal oxide as the active layer, the forming process (a step before the SET and RESET switching to initialize a soft breakdown to form a conductive filament in the device) is not required for the atomristors. A high on/off current ratio can be seen in the I-V characteristics up to > 10^6, highlighting an advantage of the crystalline monolayers over ultrathin amorphous oxides and enabling the application of multi-bit storage and neuromorphic computing.

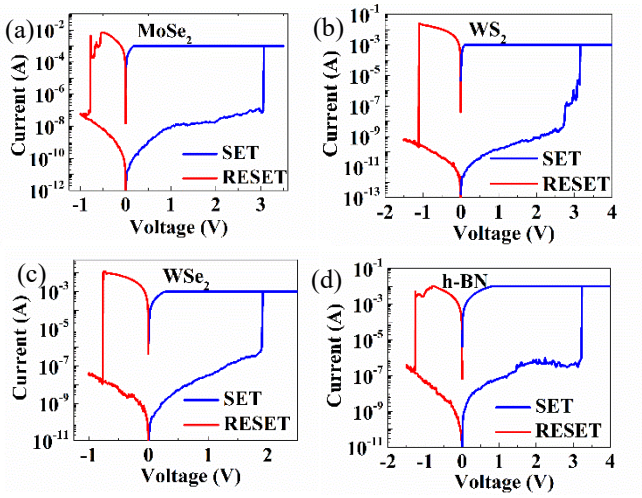

Figure 3. Representative bipolar I-V curves of $MoSe_2$, WS_2, WSe_2 and h-BN crossbar devices, indicating a universal NVRS behavior in monolayer 2D atomristors.

Other typical TMD monolayers, including $MoSe_2$, WS_2 and WSe_2, and the 2D insulator, h-BN, are also studied and show NVRS phenomenon (Fig. 3). These I-V characteristics collectively indicate a universal NVRS behavior in semiconducting and insulating 2D monolayers, which inspires the study of the intrigued mechanisms of the 2D interface system. It is worth noted that, though not shown in this paper, the TMDs and h-BN monolayer devices can work in both unipolar and bipolar configuration. Nevertheless, the underlying physics of unipolar operation is not yet fully understood. It could be due to electro-thermal heating that facilitates diffusion. A symptom of this effect is the relatively high RESET current needed to increase the local temperature to break the conductive link.

In the majority of experiments, Au was selected as an inert electrode to rule out any switching effect that might arise from interfacial metal oxide formation. Furthermore, to rule out the undesirable contribution of polymer contamination from microfabrication, very clean devices - the lithography-free and transfer-free devices (Fig. 4) were fabricated, which also produced the NVRS effect, alluding to an intrinsic origin. The lithography-free and transfer-free devices are based on monolayer MoS_2 grown directly on gold foil. Subsequently, gold top electrode is deposited using e-beam evaporation via laser shadow mask. Thus, no transfer process or lithography process is used, excluding possible residues from transfer and lithography. Similar transfer-free and litho-free devices are fabricated based on monolayer h-BN grown on Au and Ni foils, and show NVRS behavior as well.

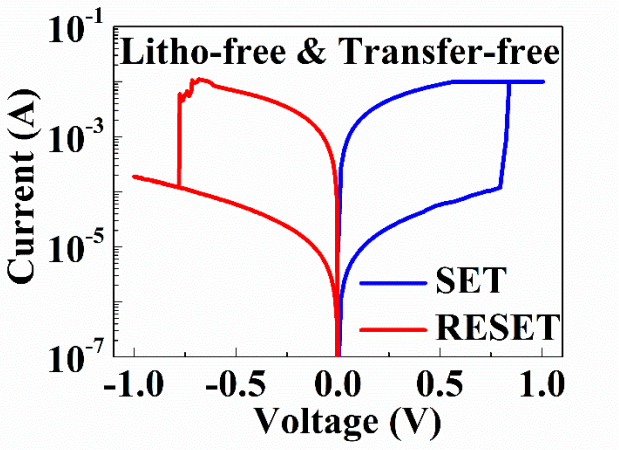

Figure 4. Representative I-V curve of clean (litho & transfer-free) Au/MoS_2/Au device, indicating an intrinsic NVRS phenomenon in 2D monolayers.

Besides the DC operation, the device can also be switched by pulse. Figure 5 shows the SET process realized by a 15-ns, 5V pulse in monolayer h-BN atomristors. The read I-V curves before and after applying the pulse clearly show the switching from OFF state to ON state with a switching speed less than 15 ns. It can be expected that with more advanced pulse generator and equipment, short switching time can be realized in the atomically thin 2D materials. With the fast switching time, the power consumption of the device can be further reduced, which is another advantage of the atomristors over other competitors.

The switching mechanism in the 2D monolayers can be explained by a local conductive-bridge-like model in the MIM sandwich. We use the h-BN with Au electrodes as an example. It can be inferred that at HRS, electrons transport through the h-BN film with boron vacancies on it, where the boron vacancies serve as trapping centers. During the SET process, the gold atoms located at the positive biased electrodes lose their electrons and become positively charged gold ions ($Au \rightarrow Au^+ + e^-$). Then, the ions are attracted by the boron vacancies and subsequently reduced ($Au^+ + e^- \rightarrow Au$), forming a conductive path in the vertical direction to establish

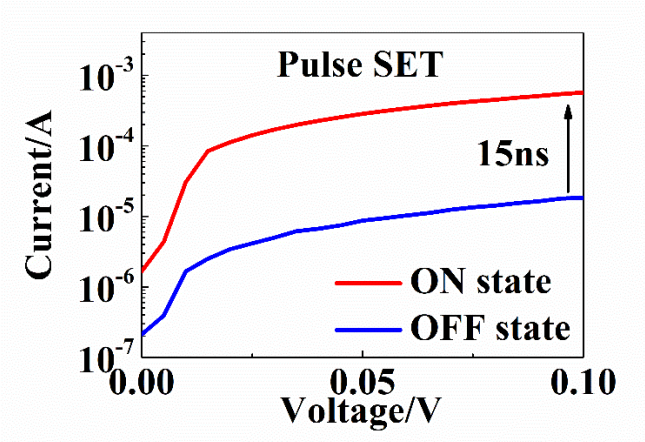

Figure 5. Read I-V curves before and after applying a 15-ns pulse to the atomritor.

the low-resistance state. The model is supported by experimental and ab-initio simulation results[11].

Applications based on the NVRS devices are studied and investigated. Non-volatile memory devices, as the most direct and promising application, can be made from the atomristors. Preliminary reliability tests have been conducted, showing stable switching characteristics. The resistance states can be retained for at least 1 month at room temperature (see Fig. 6a). For endurance, switching over 150 manual DC cycles have been achieved (Fig. 6b) with more cycles expected with further studies. At the nascent stage, the 2D atomristors have lower endurance compared with established traditional metal oxide RRAM or PCM. Though, with further research on understanding the role of material defects and interfaces, and optimized engineering of MIM devices, the device performance is expected to improve consequently while affording the benefits of atomically thin memory layer.

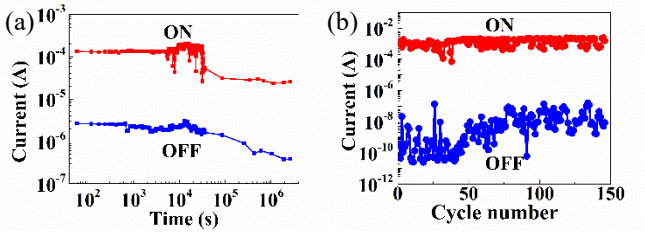

Figure 6. (a) Retention time over 1 month and (b) DC manual endurance over 150 cycles of MoS_2-based atomristors.

Non-volatile low-power RF switches represents another major application of atomristors. Contemporary switches are realized with transistor or micro-electromechanical devices, both of which are volatile with the latter also requiring large switching voltages, unideal for mobile technologies. Recently, phase-change switches have attracted interest. However, the high-temperature melting requirements and slow switching times have limited their utility. Thus, atomristors offers an unprecedented advancement for high-frequency systems owing to its low voltage operation, small form-factor, fast switching speed, and low-temperature integration compatible with Si or flexible substrates. Monolayer hBN RF switches with sub-micron dimensions showed relatively flat insertion loss less than 0.2 dB till 110 GHz (Fig. 7a). The extracted R_{ON} is ~ 1.6 Ω. The isolation performance was similarly wideband with 20 dB or higher at 100 GHz and below, and ~15dB at 110 GHz (Fig. 7b). The extracted C_{OFF} is ~ 2.3 fF. The corresponding F_{co} ~ 43 THz is more than 50% higher than non-volatile phase-change, and volatile MEMS switches[23, 24].

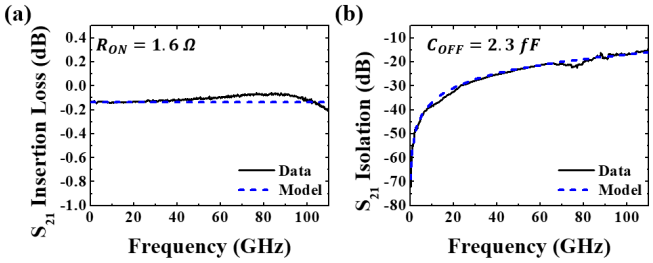

Figure 7. Measured (de-embedded) S-parameters S_{21} data in both (a) the ON (Insertion Loss), and (b) OFF (Isolation) states of RF switch. The extracted R_{ON} and C_{OFF} are 1.6 Ω and 2.3 fF, respectively. The corresponding cutoff frequency, F_{CO} is 43 THz.

CONCLUSIONS

In conclusion, the NVRS behavior is discovered in CVD-grown monolayer TMDs and h-BN in vertical MIM configuration. The minimum thickness of all NVRS materials is reduced to 0.33 nm (monolayer h-BN). The 2D atomristors show stable bipolar and unipolar resistance switching without electroforming process, large on/off current ratio (more than 10^6) and fast switching speed (< 15 ns). In the end, promising applications in memory devices and RF switches are proved based on the atomically thin 2D monolayers.

REFERENCES

[1] Akinwande, D.; Petrone, N.; Hone, J.; Nat Commun 2014, 5.
[2] Molle, A.; Goldberger, J.; Houssa, M.; Xu, Y.; Zhang, S. C.; Akinwande, D.; Nat Mater 2017, 16, 163.
[3] Tan, C. et al., Chem. Soc. Rev. 2015, vol. 44, pp. 2615-2628.
[4] Bessonov, A. A.; Kirikova, M. N.; Petukhov, D. I.; Allen, M.; Ryhänen, T.; Bailey, M. J. A. Nat Mater 2015, 14, (2), 199-204.
[5] Hao, C.; Wen, F.; Xiang, J.; Yuan, S.; Yang, B.; Li, L.; Wang, W.; Zeng, Z.; Wang, L.; Liu, Z.; Tian, Y. Advanced Functional Materials 2016, 26, (12), 2016-2024.
[6] Pan, C.; Ji, Y.; Xiao, N.; Hui, F.; Tang, K.; Guo, Y.; Xie, X.; Puglisi, F. M.; Larcher, L.; Miranda, E.; Jiang, L.; Shi, Y.; Valov, I.; McIntyre, P. C.; Waser, R.; Lanza, M. Advanced Functional Materials 2017, 1604811-n/a.
[7] Wong, H.-S. P.; Lee, H.-Y.; Yu, S.; Chen, Y.-S.; Wu, Y.; Chen, P.-S.; Lee, B.; Chen, F. T.; Tsai, M.-J. Proceedings of the IEEE 2012, 100, (6), 1951-1970.
[8] Sangwan, V. K.; Jariwala, D.; Kim, I. S.; Chen, K.-S.; Marks, T. J.; Lauhon, L. J.; Hersam, M. C. Nature Nanotechnology 2015, 10, (5), 403-406.
[9] Ge, R., et al., Nano Letters 2018, 18, (1), 434-441

[10] Ge, R., et al., 2018 IEEE International Electron Devices Meeting (IEDM), 1-5 Dec. 2018.
[11] Wu, X., et al., Advanced Materials 2019, 31, 1806790
[12] Kim, M., et al., Nature Communications (2018) 9:2524
[13] K. S. Novoselov, A. K. Geim, S. V. Morozov, D. Jiang, Y. Zhang, S. V. Dubonos, I. V. Grigorieva, A. A. Firsov Science, 22 Oct 2004 : 666-669
[14] Kin Fai Mak, Changgu Lee, James Hone, Jie Shan, and Tony F. Heinz Phys. Rev. Lett. 105, 136805
[15] Cassabois, G., Valvin, P. & Gil, B. Hexagonal boron nitride is an indirect bandgap semiconductor. Nature Photon 10, 262–266 (2016) doi:10.1038/nphoton.2015.277
[16] Meena, J.S., Sze, S.M., Chand, U. et al. Overview of emerging nonvolatile memory technologies. Nanoscale Res Lett 9, 526 (2014)
[17] Pradhan, S., Xiao, B., Mishra, S. et al. Resistive switching behavior of reduced graphene oxide memory cells for low power nonvolatile device application. Sci Rep 6, 26763 (2016)
[18] Cheng, P., Sun, K., and Hu, Y., Nano Letters 2016, 16 (1), 572-576
[19] Chang, H.-Y.; Yogeesh, M. N.; Ghosh, R.; Rai, A.; Sanne, A.; Yang, S.; Lu, N.; Banerjee, S. K.; Akinwande, D. Advanced Materials 2016, 28, (9), 1818–1823.
[20] A. Ismach, H. Chou, D. A. Ferrer, Y. P. Wu, S. McDonnell, H. C. Floresca, A. Covacevich, C. Pope, R. Piner, M. J. Kim, R. M. Wallace, L. Colombo, R. S. Ruoff, Acs Nano 2012, 6, 6378.
[21] A. C. Ismach, C.; Mende, P.; Dolocan, A.; Addou, R.; Aloni, R.; Wallace, R.; Feenstra, R.; Ruoff, R.; Colombo, L., 2d Mater 2017, 4, 025117.
[22] Z. P. Zhang, X. J. Ji, J. P. Shi, X. B. Zhou, S. Zhang, Y. Hou, Y. Qi, Q. Y. Fang, Q. Q. Ji, Y. Zhang, M. Hong, P. F. Yang, X. F. Liu, Q. Zhang, L. Liao, C. H. Jin, Z. F. Liu, Y. F. Zhang, Acs Nano 2017, 11, 4328.
[23] A. Léon, B. Reig, V. Puyal, E. Perret, P. Ferrari, and F. Podevin, "High Performance and Low Energy Consumption in Phase Change Material RF Switches," in 48th European Microwave Conference (EuMC), pp. 491-494, 2018.
[24] C.D. Patel, and G.M. Rebeiz, “A compact RF MEMS metal-contact switch and switching networks,” IEEE Microwave and Wireless Components Letters, 22(12), pp.642-644.